Monthly Notices of the Royal Astronomical Society

MNRAS **431,** 1019–1025 (2013)
Advance Access publication 2013 March 12

doi:10.1093/mnras/stt209

Caught in the act: discovery of a physical quasar triplet

E. P. Farina,[1,2⋆] C. Montuori,[1,3,4] R. Decarli[5] and M. Fumagalli[6,7†]

[1] *Università degli Studi dell'Insubria, via Valleggio 11, I-22100 Como, Italy*
[2] *INFN Milano-Bicocca–Università degli Studi di Milano-Bicocca, Piazza della Scienza 3, I-20126 Milano, Italy*
[3] *Technion, Department of Physics, IL-32000 Haifa, Israel*
[4] *Department of Physics, Faculty of Natural Sciences, University of Haifa, IL-31905 Haifa, Israel*
[5] *Max-Planck-Institut für Astronomie, Königstuhl 17, D-69117 Heidelberg, Germany*
[6] *Carnegie Observatories, 813 Santa Barbara Street, Pasadena, CA 91101, USA*
[7] *Department of Astrophysics, Princeton University, Princeton, NJ 08544-1001, USA*

Accepted 2013 January 31. Received 2013 January 7; in original form 2012 September 22

ABSTRACT

We present the discovery of a triplet of quasars at $z \approx 1.51$. The whole system is well accommodated within 25 arcsec (i.e. 200 kpc in projected distance). The velocity differences among the three objects (as measured through the broad Mg II emission line) are $<1000\ \mathrm{km\ s^{-1}}$, suggesting that the quasars belong to the same physical structure. Broad-band near-infrared (NIR) images of the field do not reveal evidence of galaxies or galaxy clusters that could act as a gravitational lens, ruling out the possibility that two or all the three quasars are multiple images of a single, strongly lensed source. QQQ J1519+0627 is the second triplet of quasars known up to date. We estimate that these systems are extremely rare in terms of simple accidental superposition. The lack of strong galaxy overdensity suggests that this peculiar system is harboured in the seeds of a yet-to-be-formed massive structure. Based on observations collected at the La Silla Observatory with the New Technology Telescope of the European Southern Observatory and at the Calar Alto Observatory with the 3.5 m telescope of the Centro Astrónmico Hispano Alemán.

Key words: quasars: general.

1 INTRODUCTION

In the current hierarchical cosmological paradigm, galaxy mergers and interactions are a major route to galaxy formation. The strong tidal fields experienced during close encounters between gas-rich systems trigger large-scale nuclear inflows that can ultimately start the activity of the supermassive black holes (SMBHs) residing in the central regions of the interacting systems (e.g. Di Matteo, Springel & Hernquist 2005). The existence of multiple, simultaneously active, SMBHs represents a key observational test for this evolutionary scenario and for our understanding of the processes regulating the quasar (QSO) activity and the co-evolution of SMBHs with their host galaxies.

A number of studies demonstrated the connection between QSOs and ultraluminous infrared galaxies that are mostly found in merging systems (e.g. Canalizo & Stockton 2001) and confirmed the signature of recent merger events in QSO hosts (e.g. Bennert et al. 2008). A noticeable example is the discovery of a spatially resolved binary QSO (projected separation pd = 21 kpc) clearly hosted by a galaxy merger (Green et al. 2010). The search for candidate binary systems of QSOs up to redshift ∼4 unveiled an enhanced QSO clustering signature at small scale ($\lesssim$50 kpc) relative to the simple extrapolation of the larger scale two-point correlation function (e.g. Hennawi et al. 2006, 2010; Myers et al. 2007, 2008; Kayo & Oguri 2012; but see Padmanabhan et al. 2009; Shen et al. 2010). This can be interpreted in terms of interactions that trigger the QSO activity (e.g. Hennawi et al. 2006; Hopkins et al. 2008). Alternatively, the small-scale excess could be a simple manifestation of the clustering properties of the haloes that host QSOs (e.g. Richardson et al. 2012).

Little is known about systems with more than two physically associated QSOs which are expected to be even more elusive objects. The only physical QSO triplet reported so far is QQQ J1432−0106 at $z = 2.076$ observed by Djorgovski et al. (2007). At smaller projected separations and lower luminosities, Liu, Shen & Strauss (2011) recently discovered a triple active galactic nucleus (AGN) in the galaxy SDSS J1027+1749 at $z = 0.066$, and Schawinski et al. (2011) serendipitously observed three low mass ($<10^7\ \mathrm{M_{\odot}}$) accreting black holes in a galaxy at $z = 1.35$.

In this paper, we present the discovery of QQQ J1519+0627, the second triplet of QSOs that is known up to date. This is the first result of our ongoing systematic search for QSO triplets among the photometric and spectroscopic data base of the Sloan Digital Sky Survey (SDSS; Aihara et al. 2011). The manuscript is organized

⋆ E-mail: emanuele.paolo.farina@gmail.com
† Hubble Fellow.

Table 1. Properties of the triple QSO systems known to date. For each QSO, we list: identification label (id), position (RA, Dec.), redshift (redshift), magnitude of the components (z, J and H), angular ($\Delta\theta$) and projected (pd) separations at the redshift of the system, and radial velocity difference (ΔV). Data for QQQ J1432−0106 are from Djorgovski et al. (2007) and the SDSS data base.

id	RA (J2000)	Dec. (J2000)	redshift	z (mag)	J (mag)	H (mag)	$\Delta\theta$ (arcsec)	pd (kpc)	ΔV (km s^{-1})
QQQ J1519+0627									
QQQ1519A	15:19:47.3	+06:27:53	1.504±0.001	18.86	18.81	18.55	$\Delta\theta(A-B)$=23.5	pd($A-B$)=198	$\Delta V(A-B)$=1100
QQQ1519B	15:19:45.7	+06:27:52	1.513±0.003	21.23	20.97	20.25	$\Delta\theta(B-C)$=3.7	pd($B-C$)=31	$\Delta V(B-C)$=850
QQQ1519C	15:19:45.9	+06:27:49	1.506±0.003	21.20	20.69	20.13	$\Delta\theta(C-A)$=21.1	pd($C-A$)=178	$\Delta V(C-A)$=250
QQQ J1432−0106									
QQQ1432A	14:32:29.2	–01:06:16	2.076	17.15	16.32	15.88	$\Delta\theta(A-B)$=5.1	pd($A-B$)=42	$\Delta V(A-B)$=280
QQQ1432B	14:32:28.9	–01:06:13	2.076	20.42	20.00	19.27	$\Delta\theta(B-C)$=3.6	pd($B-C$)=30	$\Delta V(B-C)$=100
QQQ1432C	14:32:29.2	–01:06:12	∼2.08	–	21.66	21.17	$\Delta\theta(C-A)$=4.3	pd($C-A$)=36	–

as follows. In Section 2, we describe the spectroscopic and photometric data collected in our study. The possible interpretations are discussed in Section 3, and we draw our conclusions in Section 4.

Throughout this paper, we consider a concordance cosmology with $H_0 = 70$ km s^{-1} Mpc^{-1}, $\Omega_m = 0.3$ and $\Omega_\Lambda = 0.7$. All the quoted magnitude are expressed in the AB standard photometric system (Oke 1974).

2 SELECTION AND FOLLOW-UP OBSERVATIONS

QSO multiplets observed at close projected separations are rare (e.g. Hennawi et al. 2006). Large spectroscopic surveys often fail to detect close QSO systems due to the fibre collision limits. For example, in SDSS it is not possible to obtain the spectrum for both sources in a pair with separation <55 arcsec within a single plate (Blanton et al. 2003). To overcome this limitation, we started a programme to search for close QSO triplets taking advantage of the large photometric sample of Richards et al. (2009). Three QSOs are considered a candidate triplet if (i) at least one of them has spectroscopic redshift, (ii) the other two reside within 500 kpc from it and (iii) they have coincident (within the uncertainties) photometric redshift (estimated with the procedure suggested by Weinstein et al. 2004). We selected 13 triple QSO *candidates* for spectroscopic follow up, in the redshift range $0.3 \lesssim z \lesssim 2.2$, and with an average projected separation of ∼300 kpc. Furthermore, details on the selection procedure will be provided in a forthcoming paper (Farina et al., in preparation). Here, we present the spectroscopic observations obtained for the first followed-up target among our candidates. In particular, we report our discovery of two QSOs within ∼25 arcsec from the spectroscopic QSO SDSS J151947.3+062753 (hereafter QQQ1519A; Schneider et al. 2010) and located at a similar redshift (radial velocity difference $\Delta V \lesssim 1000$ km s^{-1}).

To provide a rough estimate of the expected number of such systems, we derived the QSO three-point correlation function (ζ) from the amplitude of the two-point correlation function (ξ): $\zeta_{123}(r) = \mathcal{Q}\,[\xi_{12}(r) + \xi_{23}(r) + \xi_{31}(r)]$, where $\mathcal{Q} \approx 1$ (e.g. Peebles 1993; Djorgovski et al. 2007). Assuming the values of the projected two-point correlation function from Hennawi et al. (2006) and integrating the QSO luminosity function presented by Croom et al. (2009) above the magnitude range spanned by the photometric selected QSOs (i.e. from $M_g \approx -28.0$ to ≈ -25.5), we calculated that in a perfect survey, with no source of incompleteness, given a QSO, the probability of finding two companions within 500 kpc is $p_{\rm ABC} \approx 10^{-8}$. Out of the Schneider et al. (2010) catalogue, which consists in ∼106 000 spectroscopically confirmed QSOs in the SDSS Data Release 7 footprint, we thus expect that ∼0.002 objects have two companions. The mere observation of one (or more) systems of this kind would substantially strengthen the argument of small-scale enhancement of QSO clustering (e.g. Myers et al. 2007).

In Table 1, we list the properties of the QSOs belonging to our newly discovered triplet, labelled QQQ J1519+0627, and, for comparison, of the components of the only other triple QSO system known so far: QQQ J1432−0106. In the following paragraphs, we describe the procedures and the results of the analysis of the spectroscopic and photometric data collected on QQQ J1519+0627.

2.1 Long-slit spectroscopy

Spectra of QQQ1519B and QQQ1519C were gathered with the European Southern Observatory (ESO) Faint Object Spectrograph and Camera 2 (EFOSC2; Buzzoni et al. 1984) mounted on the New Technology Telescope (NTT) in La Silla (Chile). We performed long-slit spectroscopy on 2012 February 17, using a slit width of 1 arcsec and setting the position angle to −49°.7, so that both the QSOs were observed simultaneously. Grism #16 was used in order to continuously cover the wavelength range 6015–10320 Å with a spectral resolution $\lambda/\Delta\lambda \approx 550$ as measured on the night sky emission lines. Five frames of 900 s were acquired, for a total exposure time of 75 min on source. Standard IRAF[1] tools were used in the data reduction (bias subtraction, flat fielding, wavelength and flux calibration, spectra extraction). As flux calibrator, we observed the spectrophotometric standard star Hiltner 600. Typical residuals in the wavelength calibration are ∼1 Å.

For the analysis of the QSO spectra, we followed the procedure presented in Decarli et al. (2010b) and De Rosa et al. (2011). Namely, we model the QSO spectra with a superposition of: (i) a power-law non-thermal component; (ii) the emission of the host galaxy (adopting the elliptical galaxy model by Mannucci et al. 2001); (iii) the Fe II multiplets (from the template of Vestergaard & Wilkes 2001 and from our own original spectrum of IZw001) and (iv) the broad emission lines fitted with two Gaussian curves with the same peak wavelength (see Decarli et al. 2008). The two NTT spectra and the one from SDSS are shown in Fig. 1. A bright emission line, identified as Mg II, is observed in all the spectra at ∼7000 Å. The line identification is supported by the lack of other bright emission lines in the observed spectra, and by a tentative

[1] IRAF is distributed by the National Optical Astronomy Observatories, which are operated by the Association of Universities for Research in Astronomy, Inc., under cooperative agreement with the National Science Foundation.

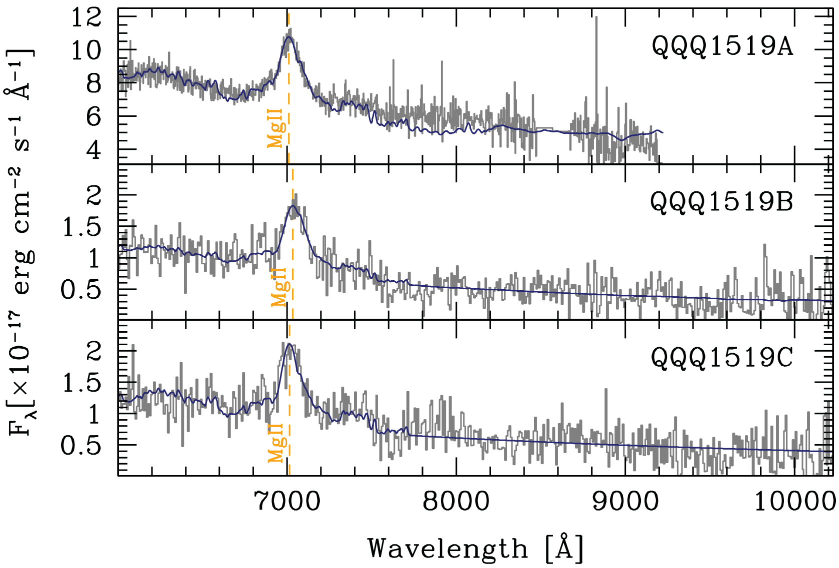

Figure 1. Spectra of the three QSOs of QQQ J1519+0627 (grey), binned by 2 pixels. The results of the fitting procedure on Mg II and Fe II lines are plotted in blue (see the text for details). The positions of the Mg II peaks are marked with orange dashed lines.

detection of the iron multiplets around the line (see our fit results in Fig. 1). These pieces of evidence firmly pin down the redshifts of the QSOs to 1.504 ± 0.001, 1.513 ± 0.003 and 1.506 ± 0.003 for A, B and C, respectively, where uncertainties are given by the positional accuracy of the Mg II line centroids.

2.2 Broad-band photometry

We gathered near-infrared (NIR) broad-band images of the QQQ J1519+0627 field using Omega2000 (Kovács et al. 2004) at the 3.5 m telescope in Calar Alto (Spain). Observations were performed on 2012 March 8 as Director Discretional Time. We observed a region of 15 arcmin × 15 arcmin around the system in z, J and H bands, i.e. sampling the rest-frame u, g and r at $z = 1.51$. We adapted usual jittering observing strategies in order to effectively subtract night sky emission. We collected 180 × 15 s frames in z (total integration time: 45 min), 18 × 100 s frames in J (total integration time: 30 min) and 36 × 50 s frames in H (total integration time: 30 min). Images were processed with our package of NIR image processing based on standard IRAF tasks. We compute the astrometric solution using the ASTROMETRY.NET software (Lang et al. 2010). Photometric calibration is achieved by comparing the photometry of field stars observed in our images with the fluxes reported in the SDSS (z-band) and 2MASS (J- and H-band) catalogues, using the following filter transformations:

$$z_{\Omega 2k} = z_{\rm SDSS} - 0.05\,(i - z)_{\rm SDSS}, \quad (1)$$

$$J_{\Omega 2k} = J_{\rm 2MASS,AB} + 0.11\,(J - H)_{\rm 2MASS,AB}, \quad (2)$$

$$H_{\Omega 2k} = H_{\rm 2MASS,AB} - 0.02\,(J - H)_{\rm 2MASS,AB}. \quad (3)$$

Equations (1)–(3) are derived by computing the spectral magnitudes of template O- to M-type stars.

The seeing during the observations was 2 arcsec (as measured on the final images), and the 5 σ limit magnitudes (computed from the rms of sky counts over a seeing area) are 23.90, 23.38 and 22.25 in z, J and H, respectively.

We use SEXTRACTOR (Bertin & Arnouts 1996) in order to identify and catalogue the sources in our images. Within the limit fluxes of our observations, we are able to study the environment of the QSO system down to $M^{\star}(z) + 1$, where $M^{\star}(z)$ is the rest-frame B-band characteristic luminosity of galaxies at redshift z as derived from the fit of the galaxy luminosity function (Ilbert et al. 2005). In order to disentangle between Galactic and extragalactic objects, we rely upon different colour–colour diagrams, also including sources from the SDSS photometric data base (see Fig. 2).

We classified a source as *star* if it is not resolved [i.e. full width at half-maximum (FWHM) $\lesssim$ seeing in all the considered images], and it lies within the locus of main sequence stars estimated through the prediction of the TRILEGAL software[2] (Girardi et al. 2005), and from the distribution of the SDSS spectroscopically confirmed stars detected also in 2MASS (Skrutskie et al. 2006). Our colour cuts are a simplified version of those adopted by Richards et al. (2002) on the SDSS photometric data base. We also check the consistency of the sources not classified as stars with the reference colours of Elliptical, Sc galaxies and QSOs obtained from the templates of Mannucci et al. (2001) and of Francis et al. (1991). In summary, in the 15 arcmin × 15 arcmin region explored, we detect 2048 sources, 807 of which are classified as star on the basis of their colours. This yields a number density of ∼3.5 stars per arcmin^2 that roughly correspond to the prediction of the TRILEGAL software in this region of the sky (∼3.1 arcmin^{-2}). The average surface density of extragalactic sources is 3.7 ± 0.2 arcmin^{-2}, that is consistent (within the uncertainties) with the 4.0 ± 0.2 arcmin^{-2} observed in the Great Observatories Origins Deep Survey (GOODS, Giavalisco et al. 2004) once we consider our z-band sensitivity limits.

3 DISCUSSION

In this section, we discuss the possible scenarios for this peculiar system.

[2] http://stev.oapd.inaf.it/cgi-bin/trilegal

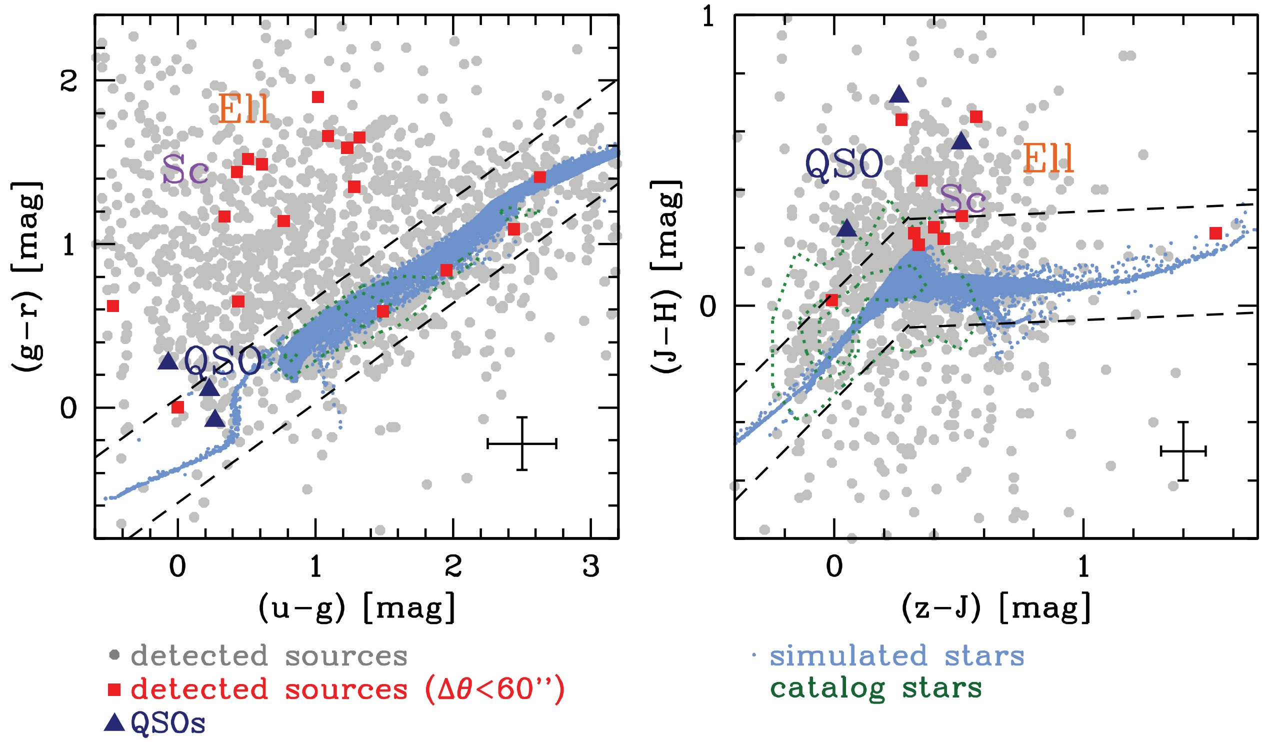

Figure 2. Colour–colour diagrams of the sources detected in the explored images (grey points). The objects within 60 arcsec from the QQQ J1519+0627 barycentre are highlighted in red. The blue triangles indicate the colours of the three QSOs of the system. Note that the number of detected sources changes, according to the different depth of each band. For comparison, we show the expected loci of Ellipticals and Sc galaxies at $z = 1$ and of QSOs at $z = 1.5$ from the template of Mannucci et al. (2001) and Francis et al. (1991). The light blue points are the star colours simulated with the TRILEGAL software (Girardi et al. 2005), and dark green contours indicate the distribution of the spectroscopically confirmed stars detected in the SDSS and 2MASS in a region of $5° \times 5°$ around the triplet, and in the GOODS survey. The black dashed lines show the colour cuts we imposed to separate stars and extragalactic objects. The crosses in the bottom right of the figures represent typical error bars on the colours.

3.1 Gravitational lens

To test the lens hypothesis for QQQ J1519+0627, we consider two different configurations: in case (i) QQQ1519B and QQQ1519C are images of the same gravitationally lensed QSO while QQQ1519A is a different QSO at similar redshift. In case (ii), also QQQ1519A is an image of the same QSO. We note that small differences are reported in the colours and in the spectra of the three QSOs (e.g. the Mg II lines peak at slightly different redshifts). This already disfavours the lensing scenario. However, due to the limited signal-to-noise ratio of the available spectra, we will focus our analysis mostly on the images.

In case (i), we model the potential well of the lensing object with a singular isothermal sphere (SIS). Multiple images of similar brightness are obtained only along the *Einstein* ring, the radius of which is parametrized as θ_E (e.g. Narayan & Schneider 1990; Chieregato, Miranda & Jetzer 2007):

$$\theta_E = 4\pi \left(\frac{\sigma}{c}\right)^2 \frac{D_{LS}}{D_S}. \tag{4}$$

Here, σ is the velocity dispersion of the SIS, c is the speed of light, D_{LS} and D_S are the angular diameter distances between the source and the lens, and between the source and the observer, respectively. The minimum value of θ_E allowed in this system corresponds to half of the separation in the sky between QQQ1519B and C, i.e. 1.85 arcsec. This implies that, for a given redshift of the lens, we can infer a lower limit for σ. If we adopt the working assumption that $\sigma = \sigma_*$ (the velocity dispersion of stars in the galaxy), we can use the Faber–Jackson relation (Faber & Jackson 1976) to convert the lower limit on σ into a luminosity limit for the lens galaxy. We use the updated version of the Faber–Jackson relation reported by Nigoche-Netro et al. (2010),

$$\log \frac{\sigma_*}{\mathrm{km\,s^{-1}}} = (-1.208 \pm 0.205) - (0.157 \pm 0.009)\, M_r, \tag{5}$$

where M_r is the rest-frame r-band absolute magnitude. We convert the observed z band into M_r using the filter- and k-corrections computed basing on the elliptical galaxy template by Mannucci et al. (2001). Fig. 3 shows that a galaxy brighter than z=19.6 is necessary to explain the observed geometry of the system in terms of strong gravitational lensing. The presence of such a galaxy is ruled out by our Omega2000 images.

Case (ii) is more extreme since wide separation lens systems are rare. In their search for lensed QSOs with angular separation less than $\Delta\theta \lesssim 20$ arcsec, Inada et al. (2008) find in the SDSS only 3 out of 22 systems with $\Delta\theta > 3$ arcsec. Hennawi, Dalal & Bode (2007) estimated that in the SDSS QSO sample there should be only a few systems ($\lesssim$4) multiply lensed by galaxy clusters with separations > 20 arcsec. Moreover, triple-imaged QSOs are not commonly observed (e.g. Lawrence et al. 1984).

The three largest separation QSO lenses known so far, SDSS J1029+2623 ($\Delta\theta$ = 22.5 arcsec, z = 2.197, Inada et al. 2006), SDSS J2222+2745 ($\Delta\theta$ = 15.1 arcsec, z = 2.82, Dahle et al. 2012) and SDSS J1004+4112 ($\Delta\theta$ = 14.6 arcsec, z = 1.734, Inada et al. 2003), have separation similar to the ones reported here. In all

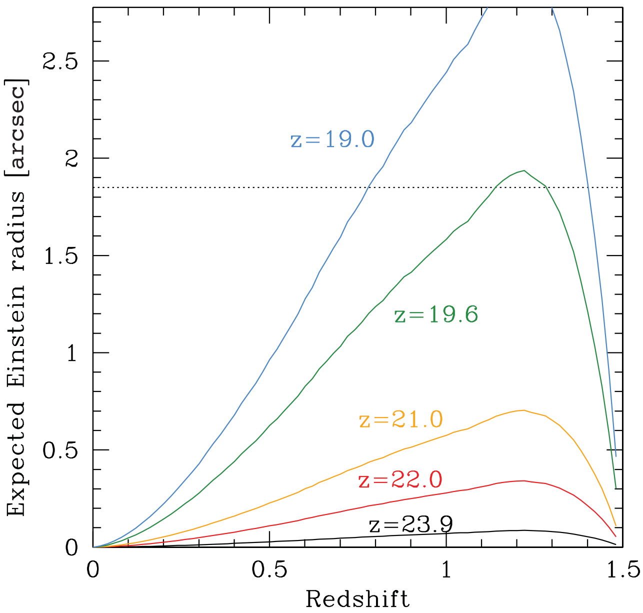

Figure 3. Expected *Einstein* ring radius for a lensing galaxy with various (observed) z-band magnitudes, as a function of redshift. The horizontal line shows the half-separation between QQQ1519B and C. The elliptical galaxy template by Mannucci et al. (2001) is used in order to compute k- and filter-corrections. We assume that the potential well of the lensing galaxy is well described by an SIS model with $\sigma = \sigma_*$, where σ_* is the stellar velocity dispersion as set by the Faber–Jackson relation (see the text for details). In the lensing scenario, a galaxy of $z \approx 19.6$ would be required in order to justify the observed separation between QQQ1519B and C. Thanks to the depth of our observations ($z_{\rm lim} \approx 23.9$), we can rule out the strong-lensing scenario for these two sources.

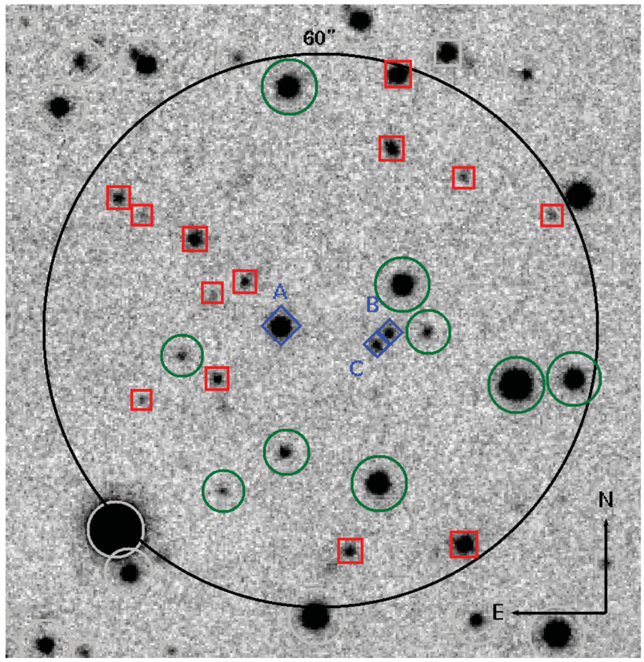

Figure 4. Image of the 60 arcsec around the triplet QQQ J1519+0627 as imaged in z band at the Calar Alto Observatory. The blue diamonds are the three QSOs. The 13 sources identified as galaxies are shown as red squares, while the nine stars as green circles. The surface densities of Galactic and extragalactic sources in this area is consistent with the detections in the rest of the image.

these cases, massive galaxy clusters act as lens (Oguri et al. 2004; Inada et al. 2006; Dahle et al. 2012). As a zeroth-order test, we estimate the velocity dispersion required to explain the separation of the images assuming again an SIS profile for the lens. As in case (i), we consider a limit for the *Einstein* radius $\theta_{\rm E} \approx 10$ arcsec that corresponds to $\sigma \approx 600$ km s^{-1} at $z \approx 0$ and $\sigma \approx 1200$ km s^{-1} at $z \approx 1$. In our image, the presence of such clusters should be apparent, but in fact the surface density of galaxies within 60 arcsec from QQQ J1519+0627 (in z band 4.1 ± 1.1 arcmin^{-2}) is consistent with those detected in the whole frame (3.7 ± 0.2 arcmin^{-2}, see Section 2.2 and Fig. 4). For instance, we consider the case that in our field was present XMMU J100750.5+125818: a galaxy cluster located at redshift $z \approx 1.08$ with a line-of-sight velocity dispersion of ~600 km s^{-1} (Schwope et al. 2010). If the cluster was centred on QQQ J1519+0627 in the first 60 arcsec, there should be at least 10 galaxies in excess to the background. This is in contrast to what is observed in the z band, where we detect only 12 galaxies instead of 22. We note that this estimate is conservative since we considered as reference only the (few) spectroscopically confirmed cluster members of XMMU J100750.5+125818, while the cluster should be more populated.

From the analysis of photometric data, we thus conclude that QQQ J1519+0627 is not a case of gravitation lens.

3.2 Chance superposition

QQQ J1519+0627 is the second triplet of QSOs at similar redshift known, after QQQ J1432−0106 (Djorgovski et al. 2007). In Section 2, we have already shown that these are extremely rare objects. Here, we estimate the expected number of QSO triplets in our sample that are originated by chance superposition of otherwise (physically) disconnected QSOs. We start from the samples of spectroscopically confirmed QSOs by Schneider et al. (2010) and the sample of photometrically selected QSO candidates by Richards et al. (2009) (both based on SDSS data), and we rely upon a procedure similar to the redshift permutation method (e.g. Osmer 1981; Zhdanov & Surdej 2001). We assume that the QSOs have the same position in the sky as in the original samples but a random redshift is assigned through a Monte Carlo simulation that takes into account the redshift distribution of our complete sample (~940 000 objects). We find that ~0.05 QSO triplets with $\Delta V <$ 2000 km s^{-1} and projected separations <200 kpc are expected. This result is an upper limit for the number of chance triple QSOs since in our computation most of the correlation was destroyed, but we kept the angular distribution of the QSOs as in the original sample.

3.3 A common physical structure

In the hypothesis that the system is virialized, the velocity differences among QQQ1519A, QQQ1519B and QQQ1519C (estimated from the broad Mg II emission line redshifts) imply a dynamical mass of $\sim 10^{13}$ M$_{\odot}$, i.e. the system would lie inside a massive structure. In order to test this scenario, we search for galaxies at redshift ~1.5 in the proximity of the system. In Fig. 5, we show the observed colour–magnitude diagram of the sources in our field. We compare the photometry of these sources with the apparent magnitude and colours of a $M^*(z)$ galaxy, where $M^*(z)$ is the characteristic luminosity (in absolute magnitudes) of galaxies at a given redshift z in the rest-frame B band, as computed by Ilbert et al. (2005). For filter- and k-corrections, we refer to the elliptical galaxy template

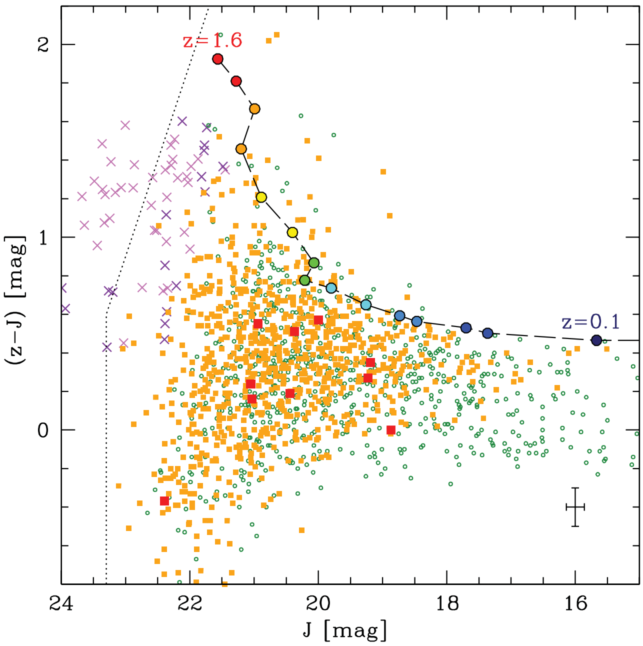

Figure 5. Observed colour–magnitude diagram for the objects detected by SEXTRACTOR in the field of QQQ J1519+0627 (green circles). The sources selected as galaxies (see Section 2.2) are shown in orange, and those that lie within 60 arcsec from the triplet are highlighted with red squares. The vertical dotted line marks the 5 σ detection limit (note that SEXTRACTOR is on average more conservative than the statistical limit magnitude). The typical error bars are shown as a cross in the bottom right of the figure. The dashed line shows the location of an $M^{\star}(z)$ galaxy at various redshifts, as derived from Ilbert et al. (2005), and assuming the elliptical galaxy template by Mannucci et al. (2001) for k-corrections. For reference, we show with light violet crosses the location of the galaxies of the galaxy cluster XMMXCS J2215.9−1738 (z = 1.46, velocity dispersion $\sigma_{\rm v}$ = 580 km s^{-1}, Stanford et al. 2006; Hilton et al. 2007, 2009). The dark violet crosses highlight the spectroscopic confirmed associations. We do not find any evidence of an overdensity of galaxies with colours consistent with a red sequence at z = 1.51, thus suggesting that the environment of QQQ J1519+0627 is not a rich cluster.

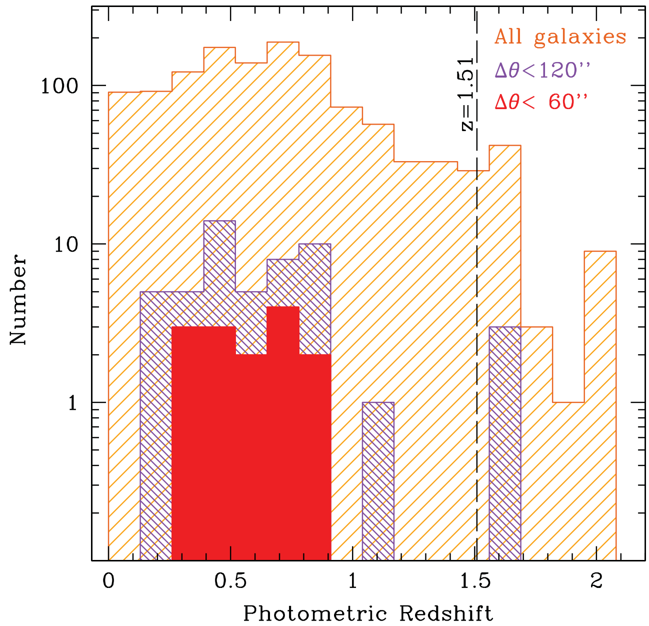

Figure 6. Distribution of the photometric redshifts estimated with HYPERZ for the galaxies selected in the field of QQQ J1519+0627 (orange histogram, see Section 3.3). The sources that reside within 120 arcsec and 60 arcsec from the triplet are shown in purple and red, respectively. The vertical dashed line marks the quasar triplet redshift. The typical errors associated with the photometric redshift determination are ~0.2. None of the galaxies close to QQQ J1519+0627 have a SED consistent with that of a galaxy at z ~ 1.5, confirming that there is no strong galaxy overdensity around the quasar triplet.

by Mannucci et al. (2001). We do not find evidence of a strong overdensity of sources with colours consistent with those of a red sequence at $z \approx 1.5$. This suggests that QQQ J1519+0627 is not located in a rich galaxy cluster or that the red sequence is not yet formed. We also estimate the photometric redshifts of the sources in the field of QQQ J1519+0627 with HYPERZ[3] (Bolzonella, Miralles & Pelló 2000) relying upon different galaxy templates (i.e. starburst, elliptical, lenticular, different type of spirals and irregular galaxies) and assuming the extinction law by Calzetti et al. (2000). It is worth noting that this choice of dust extinction model has only marginal effects on our results. This analysis confirms that none of the objects detected within 60 arcsec (that corresponds to ~500 kpc at the triplet redshift) and 120 arcsec (~1 Mpc) have colours consistent with a galaxy at z ~ 1.5 (see Fig. 6). We thus propose that the physical structure, where the three QSOs reside, may be caught in the act of formation (similarly to what reported in e.g.: Decarli, Reynolds & Dotti 2009; Decarli et al. 2010a; Farina, Falomo & Treves 2011).

[3] http://webast.ast.obs-mip.fr/hyperz/

4 CONCLUSIONS

We report the discovery of a triplet of QSOs with angular separations between 3.7 and 23.5 arcsec at a similar redshift of $z \approx 1.5$. The three sources have relative velocities within ~1000 km s^{-1} as derived from our measurements of the Mg II broad emission line and of the surrounding Fe II multiplets in the observed optical spectra. From the analysis of u, g, r, i, z, J and H broad-band images, we conclude that this system consist of three distinct sources rather than being a multiply imaged lensed QSO. This would be the second triplet of QSOs discovered so far after QQQ J1432−0106 (Djorgovski et al. 2007). We estimate that the probability that these systems are due to chance superposition are negligible. No clear galaxy overdensity is reported at photometric redshift consistent with the one of the triplet. We therefore propose that these systems are part of an ongoing common physical structure formation.

The projected separation of QQQ1519A from the other two members of the system is greater than the typical distances between interacting systems (~50 kpc; e.g. Hennawi et al. 2006; Foreman, Volonteri & Dotti 2009). This implies that the observed nuclear activity of QQQ1519A was probably not triggered during an interaction involving the three systems at the same time. On the other hand, due to the smaller separation observed between QQQ1519B and C, the triggering of nuclear activity by galactic interactions may be a viable scenario for these QSOs. More conclusive constraints on the dynamics of this peculiar system and on the properties of its environment will be obtained from future higher signal-to-noise ratio spectroscopic data in the NIR band and deeper photometric images.

ACKNOWLEDGEMENTS

We thank the Calar Alto staff for the generous allocation of DDT time and the prompt execution of our programme. We acknowledge A. Treves for helpful suggestions and comments on the manuscript. For this work EPF was supported by Società Carlo Gavazzi S.p.A. and by Thales Alenia Space Italia S.p.A. RD acknowledges funding from Germany's National Research Centre for Aeronautics and Space (DLR, project FKZ 50 OR 1104). Support for MF was provided by NASA through Hubble Fellowship grant HF-51305.01-A awarded by the Space Telescope Science Institute, which is operated by the Association of Universities for Research in Astronomy, Inc., for NASA, under contract NAS 5-26555. For this work, we use: (i) spectra from ESO/NTT Telescope in La Silla; (ii) imaging from Centro Astrónmico Hispano Alemán (CAHA)/3.5 m Telescope and (iii) data from the Sloan Digital Sky Survey. Funding for SDSS-III has been provided by the Alfred P. Sloan Foundation, the Participating Institutions, the National Science Foundation and the U.S. Department of Energy Office of Science. The SDSS-III web site is http://www.sdss3.org/. SDSS-III is managed by the Astrophysical Research Consortium for the Participating Institutions of the SDSS-III Collaboration including the University of Arizona, the Brazilian Participation Group, Brookhaven National Laboratory, University of Cambridge, University of Florida, the French Participation Group, the German Participation Group, the Instituto de Astrofisica de Canarias, the Michigan State/Notre Dame/JINA Participation Group, Johns Hopkins University, Lawrence Berkeley National Laboratory, Max Planck Institute for Astrophysics, New Mexico State University, New York University, Ohio State University, Pennsylvania State University, University of Portsmouth, Princeton University, the Spanish Participation Group, University of Tokyo, University of Utah, Vanderbilt University, University of Virginia, University of Washington and Yale University.

REFERENCES

Aihara H. et al., 2011, ApJS, 193, 29
Bennert N., Canalizo G., Jungwiert B., Stockton A., Schweizer F., Peng C., Lacy M., 2008, in Bureau M., Athanassoula E., Barbuy B., eds, Proc. IAU Symp. 245, Formation and Evolution of Galaxy Bulges. Cambridge Univ. Press, Cambridge, p. 235
Bertin E., Arnouts S., 1996, A&AS, 117, 393
Blanton M. R., Lin H., Lupton R. H., Maley F. M., Young N., Zehavi I., Loveday J., 2003, AJ, 125, 2276
Bolzonella M., Miralles J.-M., Pelló R., 2000, A&A, 363, 476
Buzzoni B. et al., 1984, Messenger, 38, 9
Calzetti D., Armus L., Bohlin R. C., Kinney A. L., Koornneef J., Storchi-Bergmann T., 2000, ApJ, 533, 682
Canalizo G., Stockton A., 2001, ApJ, 555, 719
Chieregato M., Miranda M., Jetzer P., 2007, A&A, 474, 777
Croom S. M. et al., 2009, MNRAS, 399, 1755
Dahle H. et al., 2012, preprint (arXiv:1211.1091)
De Rosa G., Decarli R., Walter F., Fan X., Jiang L., Kurk J., Pasquali A., Rix H. W., 2011, ApJ, 739, 56
Decarli R., Labita M., Treves A., Falomo R., 2008, MNRAS, 387, 1237
Decarli R., Reynolds M. T., Dotti M., 2009, MNRAS, 397, 458
Decarli R., Falomo R., Treves A., Barattini M., 2010a, A&A, 511, A27
Decarli R., Falomo R., Treves A., Kotilainen J. K., Labita M., Scarpa R., 2010b, MNRAS, 402, 2441
Di Matteo T., Springel V., Hernquist L., 2005, Nat, 433, 604
Djorgovski S. G., Courbin F., Meylan G., Sluse D., Thompson D., Mahabal A., Glikman E., 2007, ApJ, 662, L1
Faber S. M., Jackson R. E., 1976, ApJ, 204, 668
Farina E. P., Falomo R., Treves A., 2011, MNRAS, 415, 3163
Foreman G., Volonteri M., Dotti M., 2009, ApJ, 693, 1554
Francis P. J., Hewett P. C., Foltz C. B., Chaffee F. H., Weymann R. J., Morris S. L., 1991, ApJ, 373, 465
Giavalisco M. et al., 2004, ApJ, 600, L93
Girardi L., Groenewegen M. A. T., Hatziminaoglou E., da Costa L., 2005, A&A, 436, 895
Green P. J., Myers A. D., Barkhouse W. A., Mulchaey J. S., Bennert V. N., Cox T. J., Aldcroft T. L., 2010, ApJ, 710, 1578
Hennawi J. F. et al., 2006, AJ, 131, 1
Hennawi J. F., Dalal N., Bode P., 2007, ApJ, 654, 93
Hennawi J. F. et al., 2010, ApJ, 719, 1672
Hilton M. et al., 2007, ApJ, 670, 1000
Hilton M. et al., 2009, ApJ, 697, 436
Hopkins P. F., Hernquist L., Cox T. J., Kereš D., 2008, ApJS, 175, 356
Ilbert O. et al., 2005, A&A, 439, 863
Inada N. et al., 2003, Nat, 426, 810
Inada N. et al., 2006, ApJ, 653, L97
Inada N. et al., 2008, AJ, 135, 496
Kayo I., Oguri M., 2012, MNRAS, 424, 1363
Kovács Z., Mall U., Bizenberger P., Baumeister H., Röser H.-J., 2004, Proc. SPIE, 5499, 432
Lang D., Hogg D. W., Mierle K., Blanton M., Roweis S., 2010, AJ, 139, 1782
Lawrence C. R., Schneider D. P., Schmidt M., Bennett C. L., Hewitt J. N., Burke B. F., Turner E. L., Gunn J. E., 1984, Sci, 223, 46
Liu X., Shen Y., Strauss M. A., 2011, ApJ, 736, L7
Mannucci F., Basile F., Poggianti B. M., Cimatti A., Daddi E., Pozzetti L., Vanzi L., 2001, MNRAS, 326, 745
Myers A. D., Brunner R. J., Richards G. T., Nichol R. C., Schneider D. P., Bahcall N. A., 2007, ApJ, 658, 99
Myers A. D., Richards G. T., Brunner R. J., Schneider D. P., Strand N. E., Hall P. B., Blomquist J. A., York D. G., 2008, ApJ, 678, 635
Narayan R., Schneider P., 1990, MNRAS, 243, 192
Nigoche-Netro A., Aguerri J. A. L., Lagos P., Ruelas-Mayorga A., Sánchez L. J., Machado A., 2010, A&A, 516, 96
Oguri M. et al., 2004, ApJ, 605, 78
Oke J. B., 1974, ApJS, 27, 21
Osmer P. S., 1981, ApJ, 247, 762
Padmanabhan N., White M., Norberg P., Porciani C., 2009, MNRAS, 397, 1862
Peebles P. J. E., 1993, Principles of Physical Cosmology. Princeton Univ. Press, Princeton, NJ
Richards G. T. et al., 2002, AJ, 123, 2945
Richards G. T. et al., 2009, ApJS, 180, 67
Richardson J., Zheng Z., Chatterjee S., Nagai D., Shen Y., 2012, ApJ, 755, 30
Schawinski K., Urry M., Treister E., Simmons B., Natarajan P., Glikman E., 2011, ApJ, 743, L37
Schneider D. P. et al., 2010, AJ, 139, 2360
Schwope A. D. et al., 2010, A&A, 513, L10
Shen Y. et al., 2010, ApJ, 719, 1693
Skrutskie M. F. et al., 2006, AJ, 131, 1163
Stanford S. A. et al., 2006, ApJ, 646, L13
Vestergaard M., Wilkes B. J., 2001, ApJS, 134, 1
Weinstein M. A. et al., 2004, ApJS, 155, 243
Zhdanov V. I., Surdej J., 2001, A&A, 372, 1

This paper has been typeset from a TEX/LATEX file prepared by the author.